

Figure S1. GPC effluent curve of the PHEAA dissolved in DMSO.

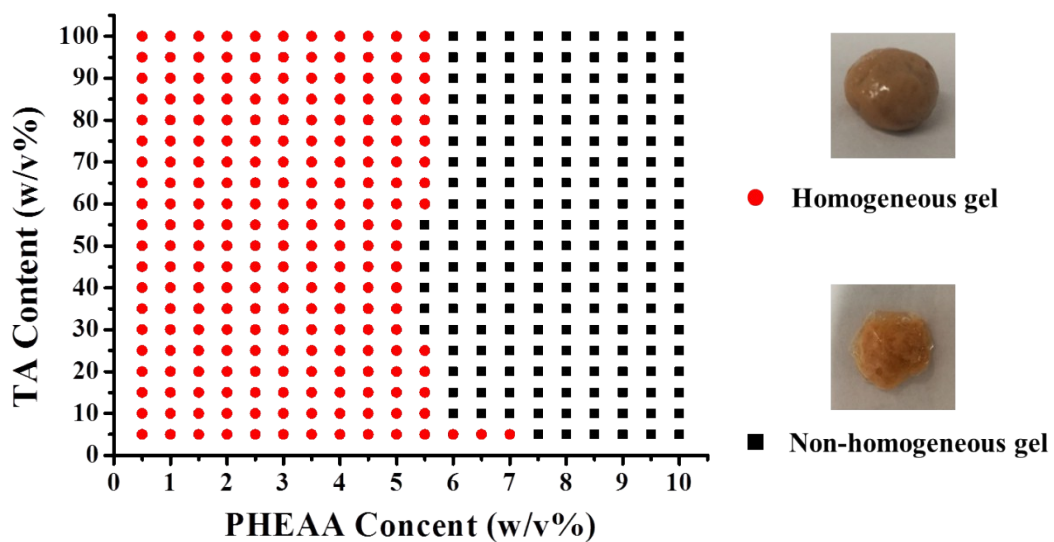


Figure S2. Phase diagram of the hydrogels prepared with different TA and PHEAA polymer concentrations.

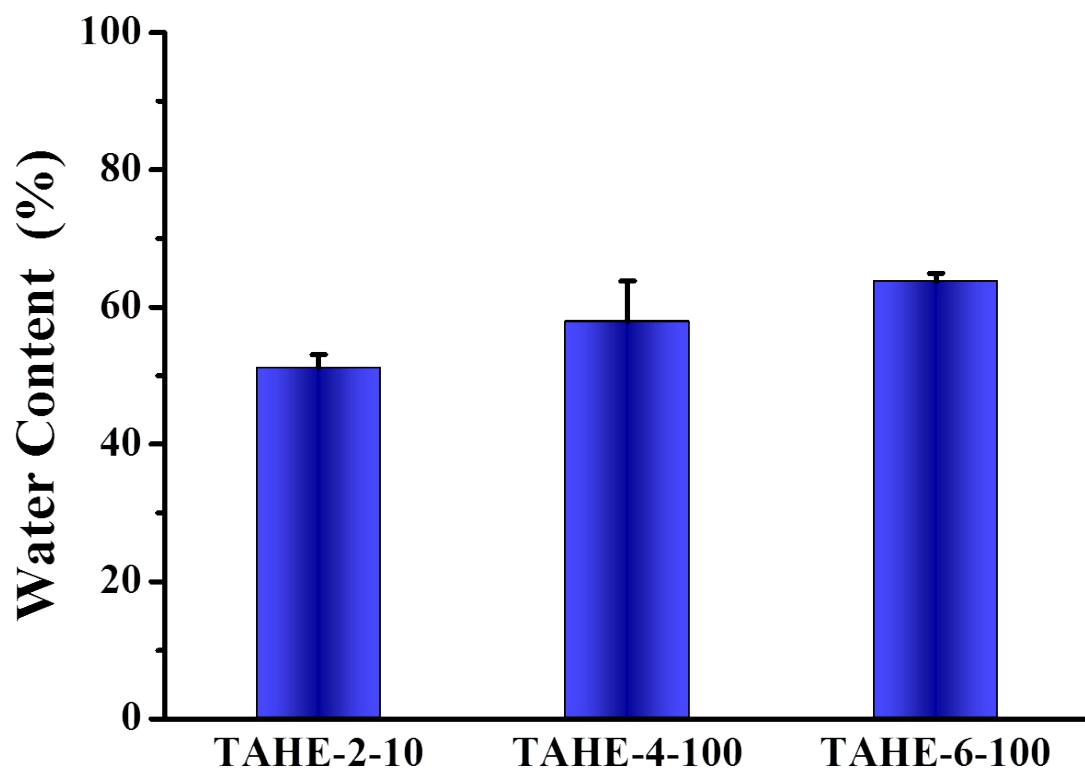


Figure S3. Water content of TAHE hydrogels prepared with different PHEAA concentrations.

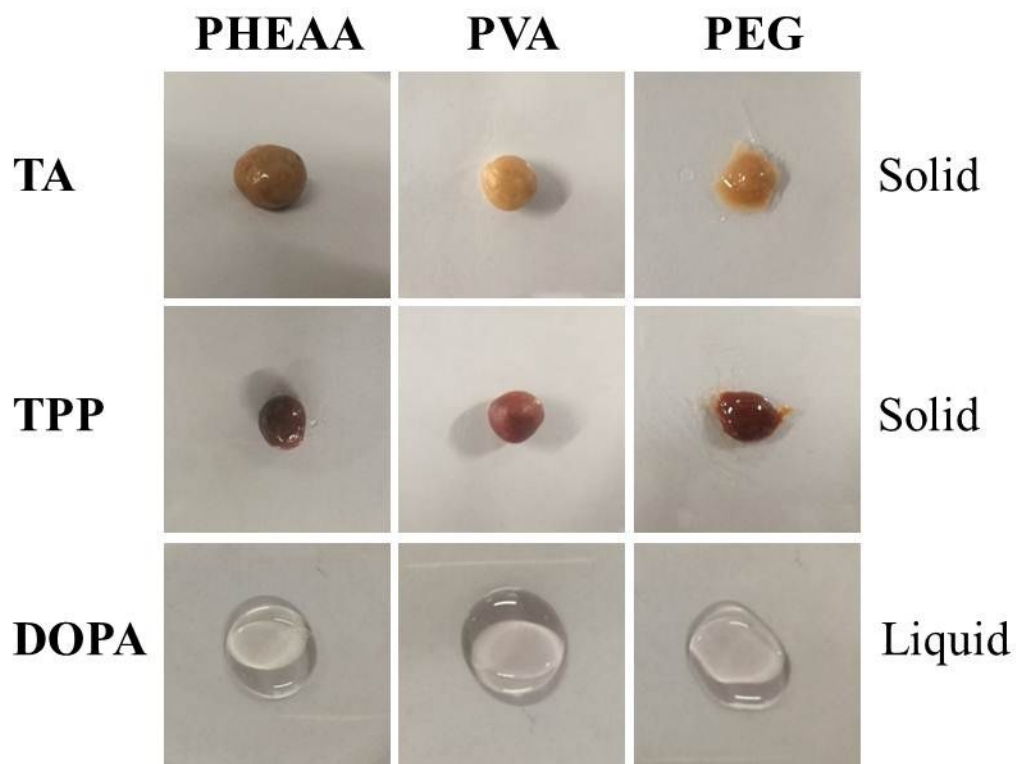


Figure S4. Digital photos showing the macroscopic state of three polyphenol substances mixed

with different polymer solutions.

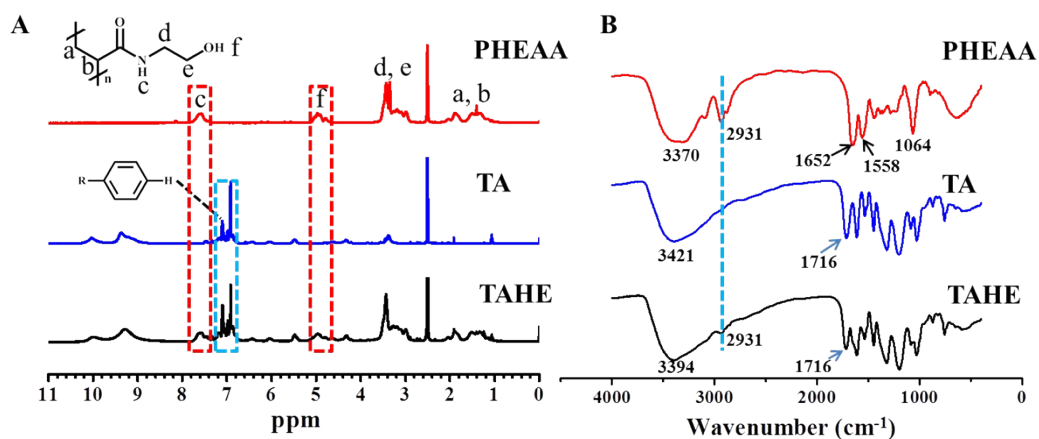


Figure S5.  $^1\text{H}$ NMR spectra of PHEAA, TA, and TAHE in DMSO- $d_6$  (A). FTIR spectra of PHEAA, TA, and TAHE (B).

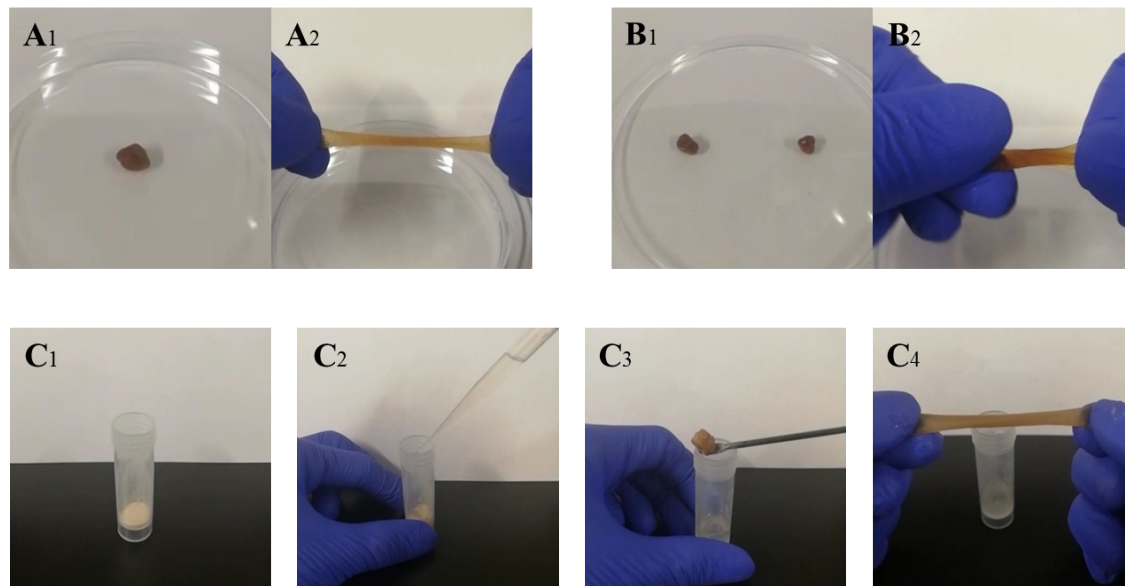


Figure S6. Digital photos of stretching shape (A). self-healing process of the TAHE hydrogel (B). and the re-formation of the TAHE hydrogel after rehydration (C).

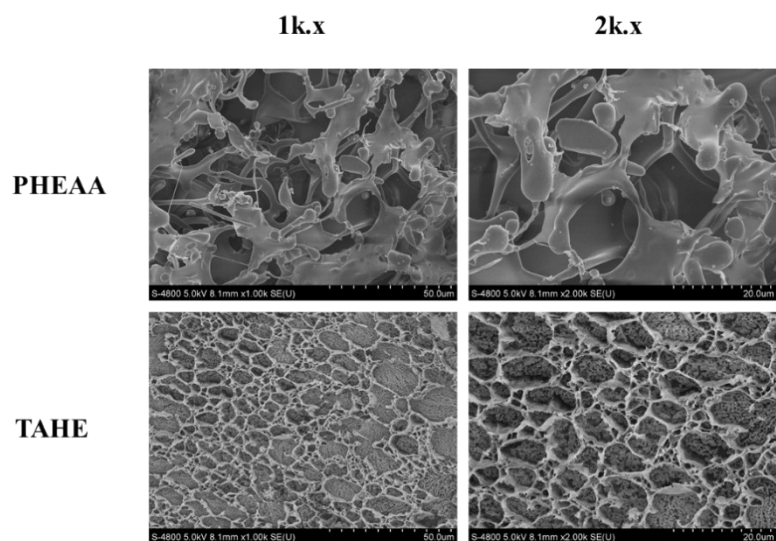


Figure S7. SEM images of the freeze-dried PHEAA and TAHE hydrogel.

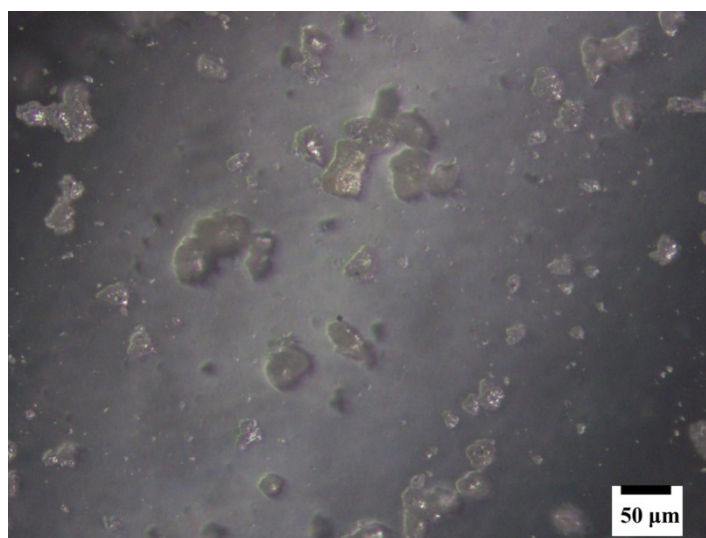


Figure S8. Optical micrograph of TAHE powder.

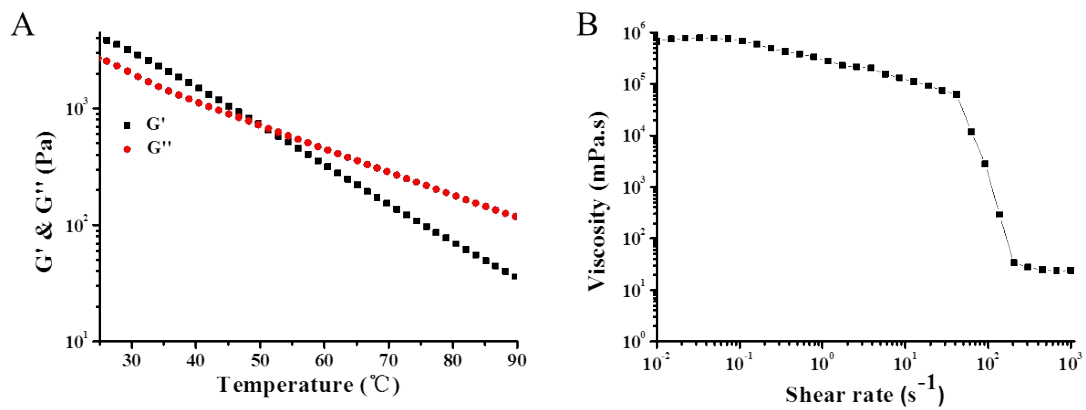


Figure S9. Storage moduli  $G'$  and loss moduli  $G''$  in a temperature amplitude sweep test (A). Viscosity change of the TAHE hydrogel as a function of shear rate (B).

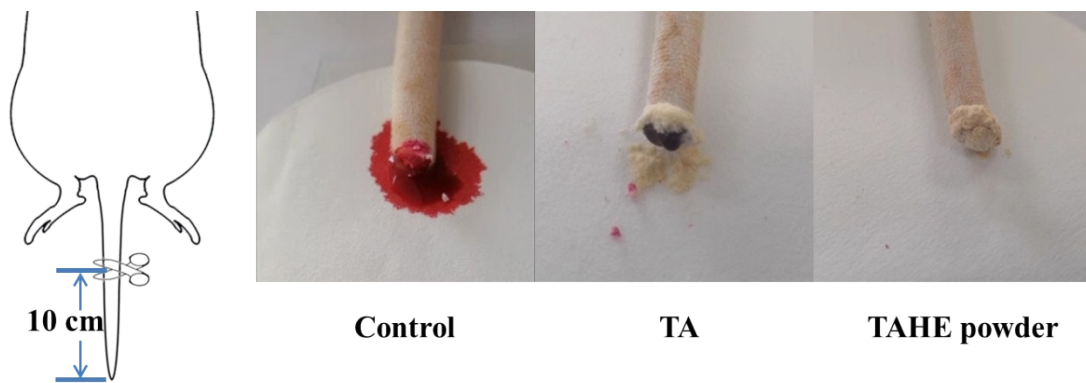


Figure S10. Scheme of the rat tail amputation model and digital images of hemostasis of amputated rats' tail treated by TA and TAHE powder.

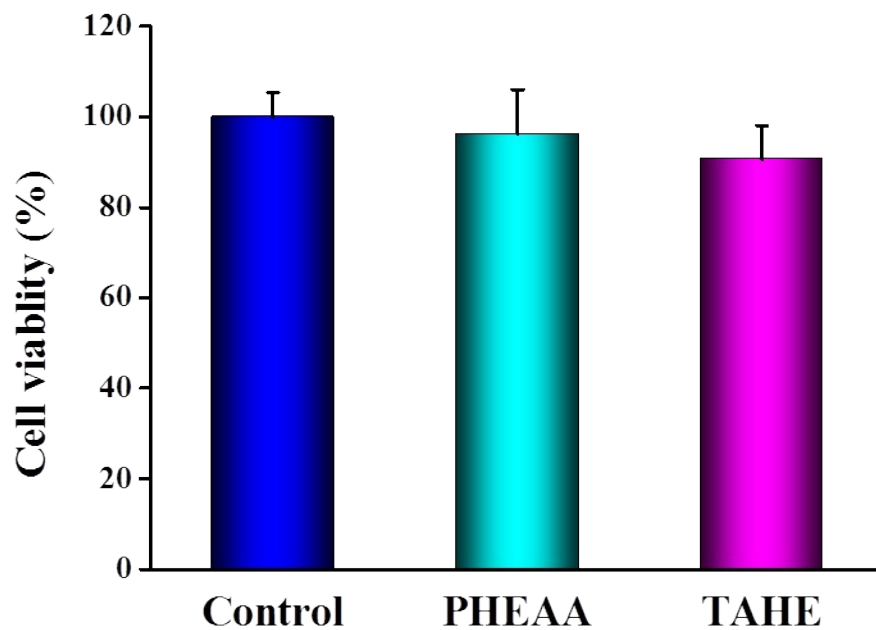


Figure S11. Cell viability of L929 cell after incubating with the extraction solution of PHEAA and TAHE hydrogels.

**Video S1:** The coacervate hydrogel can be stretched from a spherical shape into a flat sheet.

**Video S2:** After cutting it into two halves by a scalpel, the two fragments of the coacervate hydrogel completely merge to a whole gel through simply kneading for a few seconds without any other external stimuli.

**Video S3:** The coacervate hydrogel powder can fuse together to form a whole gel again when it is rehydrated, and the fused hydrogel is extensible.

**Video S4:** The hemostatic performance of TAHE the powder is evaluated on rat liver bleeding model. No treatment is used as a control group.